A Novel Position Sensorless Speed Control Scheme for Permanent Magnet Synchronous Motor Drives

Tae-Hyun Won and Man Hyung Lee

Abstract - PMSMs (permanent magnet synchronous motors) are widely used in industrial applications and home appliances because of their high torque to inertia ratio, superior power density, and high efficiency. For high performance control, accurate informations about the rotor position is essential. Sensorless algorithms have lately been studied extensively due to the high cost of position sensors and their low reliability in harsh environments. A novel position sensorless speed control for PMSMs uses indirect flux estimation and is presented in this paper. Rotor position and angular velocity are estimated by the proposed indirect flux estimation. Linkage flux and magnetic field flux are calculated by the voltage equations and the measured phase current without any integration. Instead of linkage flux calculation with integral operation, indirect flux and differential magnetic field are used for the estimation of rotor position. A proper rejection technique for current noise effect in the calculation of differential linkage flux is introduced. The proposed indirect flux detecting method is free from the integral rounding error and linkage flux drift problem, because differential linkage flux can be calculated without any integral operation. Furthermore, electrical parameters of the PMSM can be measured by the proposed TCM (time compression method) for soft starting and precise estimation of rotor position. The position estimator uses accurate electrical parameters that are obtained from the proposed TCM at starting strategy. In the operating region, a proper compensation method for temperature effect can compensate for the estimation error from the variation of electrical parameters. The proposed novel position sensorless speed control scheme is verified by the experimental results.

Keyword - PMSM, sensorless, indirect flux estimation, time compression method

1. Introduction

Permanent magnet synchronous motors are widely used in industrial applications and home appliances because of their high torque, efficiency, and superior power density. Since a complex control algorithm can be easily implemented with the development of power electronics and microprocessors, the use of PMSMs has dramatically increased. Electrical commutation of PMSMs is implemented according to the rotor position. For the proper control of PMSMs, accurate information about rotor position is essential. Most variable speed drive with PMSMs use position information from the rotary shaft sensor, such as the optical encoder, resolver, and magnetic hall sensor. In many industrial applications, the presence of a shaft sensor may substantially reduce the overall ruggedness of the drive. Furthermore, the reliability of the position sensor is reduced in harsh environments. In others, the position sensor may add significantly to the drive cost. Because of these drawbacks, shaft position sensorless techniques are a popular topic of study [1]-[6].

This paper proposes an indirect flux detecting method for the accurate position estimation of PMSMs. Instead of linkage flux calculation with integral operation, indirect flux and a differential magnetic field are used for the estimation of rotor position. A proper rejection technique for current noise effect in the calculation of differential linkage flux is introduced. The proposed indirect flux detecting method is free from the integral rounding error and linkage flux drift problem because differential linkage flux can be calculated without any integral operation.

For the accurate estimation of rotor position and higher control performance, precise information of electrical parameters is essential. This paper introduces a TCM (time compression method) for the on-line measurement of motor parameters. The TCM uses the time-extended phase current of the PMSM and test pulse voltage. Fast fourier transformation (FFT) analysis of the measured signals and least mean square (LMS) can detect an accurate electrical parameters of PMSM at any starting point. For the recovery of the original measured signal, time compression with inverse function in frequency domain is used. A digital signal processing (DSP) controller can detect accurate electrical parameters at any starting instant with the proposed TCM.

A simple estimation algorithm with the proposed indirect flux detection and TCM can produce an accurate rotor position information. In addition, parameter fluctuation due to temperature variation is predicted and compensated for to guarantee the performance.

Various experimental results show the effectiveness of

Manuscript received: May 21, 2002 accepted: June 3, 2002
Tae-Hyun Won is with Dongeui Institute of Technology, Korea.
Man Hyung Lee is with Pusan National University, Korea.

the proposed sensorless speed control from standstill to rated speed region.

2. Proposed Sensorless Algorithm

2.1 The Mathematical Modeling of the PMSM

In the mathematical modeling of the PMSMs, a permanent magnet is represented by the field winding with constant current. With the assumption of a cylindrical rotor, saliency can be ignored.

Fig. 1 shows the equivalent circuit of the PMSM in the stationary reference frame.

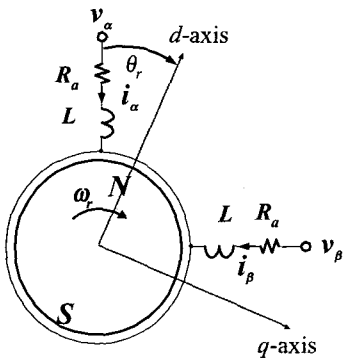

Fig. 1 The equivalent circuit of the PMSM in the stationary reference frame

In Fig. 1, the cylindrical rotor with a permanent magnet is represented by N and S and rotates clock-wise with angular velocity ω_r. The d-q axis in Fig. 1 denotes the direct and quadrature directions of the magnetic field.

The instantaneous voltage equation of the equivalent circuit of the PMSM in the stationary reference frame can be express as follows[2]-[3].

$$v_{\alpha\beta} = R \cdot i_{\alpha\beta} + p \cdot \lambda_{\alpha\beta} \tag{1}$$

where $v_{\alpha\beta}, i_{\alpha\beta}$: voltage and current in α-β axis
$\lambda_{\alpha\beta}$: linkage flux in α-β axis
p : differential operator.

With the magnetic field flux λ_M, linkage flux of PMSM can be expressed as follows in the stationary reference frame.

$$\begin{aligned} \lambda_\alpha &= Li_\alpha + \lambda_{M\alpha} \\ \lambda_\beta &= Li_\beta + \lambda_{M\beta} \end{aligned} \tag{2}$$

where $\lambda_{M\alpha}$ and $\lambda_{M\beta}$ denote the magnetic field by the permanent magnet in stationary reference frame and can be represented as a function of rotor position θ_r.

$$\begin{aligned} \lambda_{M\alpha} &= \lambda_M \cos(\theta_r) \\ \lambda_{M\beta} &= \lambda_M \sin(\theta_r) \end{aligned} \tag{3}$$

2.2 Indirect Flux Detecting Method

As shown in Eqs.(2)-(3), linkage flux of the PMSM contains rotor position information. From the relationship of rotor position and linkage flux, most sensorless algorithms use the linkage flux calculation [4]-[5]. However, linkage flux of PMSM has been derived by the integral operation as shown in Eq.(1). The initial error of integration and the drift problem are significant in the estimation of rotor position. Therefore, this paper proposes indirect flux detecting with differential magnetic field.

Fig. 2 shows the space vector diagram of flux linkage and magnetic field in stationary reference frame.

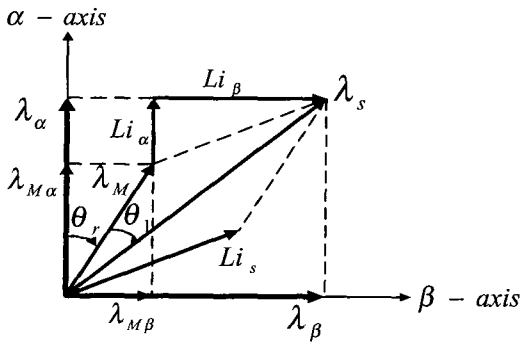

Fig. 2 Space vector diagram of flux linkage

The angle θ_l denotes load angle between linkage flux λ_s and magnetic field λ_M. The load angle depends on the load condition of the PMSM and the constant in steady state.

From the space vector diagram of Fig. 2, the linkage flux of PMSM can be expressed as follows.

$$\begin{aligned} \lambda_\alpha &= |\lambda_s| \cos(\theta_r + \theta_1) \\ \lambda_\beta &= |\lambda_s| \sin(\theta_r + \theta_1) \end{aligned} \tag{4}$$

where $|\lambda_s| = \sqrt{\lambda_\alpha^2 + \lambda_\beta^2}$.

From Eqs.(2)-(4), the differential linkage flux and magnetic field can be derived as follows.

$$\begin{aligned} p\lambda_\alpha &= -\omega_r |\lambda_s| \sin(\theta_r + \theta_1) \\ p\lambda_\beta &= \omega_r |\lambda_s| \cos(\theta_r + \theta_1) \end{aligned} \tag{5}$$

$$\begin{aligned} p\lambda_{M\alpha} &= -\omega_r |\lambda_M| \sin(\theta_r) \\ p\lambda_{M\beta} &= \omega_r |\lambda_M| \cos(\theta_r) \end{aligned} \tag{6}$$

where $\omega_r = \frac{d}{dt}\theta_r$, $\omega_r' = \frac{d}{dt}(\theta_r + \theta_1)$.

From the differential linkage flux and magnetic field, the instantaneous angular speed of the rotor can be derived.

In this paper, the magnetic field of the PMSM in the stationary reference frame are estimated from the instantaneous voltage equation, Eqs.(1) and electrical parameters. The estimated magnetic field and differential magnetic field can be estimated as follows.

$$\begin{aligned} \hat{\lambda}_{M\alpha} &= \hat{\lambda}_{M\alpha}(\hat{\theta}_r) \\ \hat{\lambda}_{M\beta} &= \hat{\lambda}_{M\beta}(\hat{\theta}_r) \end{aligned} \tag{7}$$

$$\begin{aligned} p\hat{\lambda}_{M\alpha} &= v_\alpha - R_a i_\alpha - pLi_\alpha \\ p\hat{\lambda}_{M\beta} &= v_\beta - R_a i_\beta - pLi_\beta \end{aligned} \tag{8}$$

where $\hat{\theta}_r$ is the estimated rotor position.

The differential magnetic field can be obtained via the relationship of applied voltage and voltage drops in winding resistance and inductance. However, estimation of differential magnetic flux requires the differential of the current. In detected phase currents, the harmonic component consists of PWM switching. For stable estimation of the proposed indirect flux method, the voltage drop in winding inductance must be obtained by the rejection of the direct differential of the phase current. In this paper, differential current is calculated using current vector and estimated rotor speed.

At first, the measured phase current from the low pass filter (LPF) can be expressed as

$$i_{\alpha\beta} = I_p \angle \theta_i \tag{9}$$

where $I_p = \sqrt{(i_\alpha)^2 + (i_\beta)^2}$

$$\theta_i = \tan^{-1}\left(\frac{i_\alpha}{i_\beta}\right).$$

For simple calculation, this paper uses a normalized arcsine table of current vector rather than of arctangent, as

$$\theta_i = \sin^{-1}\left(\frac{i_\alpha}{I_p}\right). \tag{10}$$

From Eqs.(9)-(10), the voltage drop in winding inductance can be easily estimated by the rejection of direct differential calculation.

$$\begin{aligned} pLi_\alpha &= LI_p\hat{\omega}_r \sin(\theta_i) \\ pLi_\beta &= LI_p\hat{\omega}_r \cos(\theta_i) \end{aligned} \tag{11}$$

The instantaneous angular velocity can be derived from the estimation of magnetic flux.

$$\hat{\omega}_h = sgn(\hat{\omega}_r)\frac{\sqrt{(p\hat{\lambda}_{M_\alpha})^2 + (p\hat{\lambda}_{M_\beta})^2}}{\lambda_M} \tag{12}$$

To compensate for the estimation error from the nonlinear characteristics of the voltage equation, compensation term is a function of the estimated position and angular velocity. The error term is for the continuous compensation of the estimation error and robust sensorless control.

$$\begin{aligned} \varepsilon_\alpha &= p\hat{\lambda}_{M\alpha} + \lambda_M\hat{\omega}_r \sin(\hat{\theta}_r) \\ \varepsilon_\beta &= p\hat{\lambda}_{M\beta} - \lambda_M\hat{\omega}_r \cos(\hat{\theta}_r) \end{aligned} \tag{13}$$

$$\varepsilon = sgn(\hat{\omega}_r)\sqrt{(\varepsilon_\alpha)^2 + (\varepsilon_\beta)^2} \tag{14}$$

From Eqs.(12)-(14) the proposed indirect flux method estimated angular velocity and rotor position can be derived as.

$$\hat{\omega}_r = \hat{\omega}_h + (K_p\varepsilon + K_i\int \varepsilon dt) \tag{15}$$

$$\hat{\theta}_r = \hat{\theta}_r(0) + \int \hat{\omega}_r(t)\,dt \tag{16}$$

where K_p, K_i : the PI gain of compensator and
$\hat{\theta}_r(0)$: initial estimated rotor position.

Fig. 3 shows the block diagram of the proposed sensorless estimation.

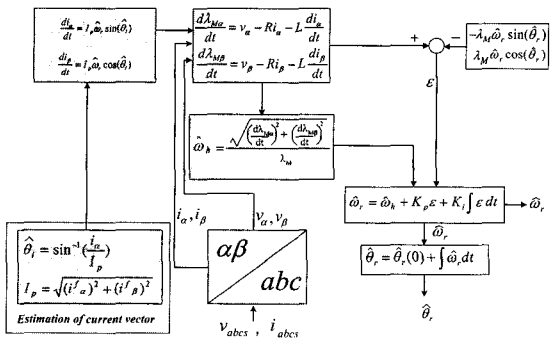

Fig. 3 Block diagram of proposed sensorless algorithm

3. Parameter Measurement and Compensation

3.1 Parameter Measurement using TCM

The proposed sensorless algorithm uses only electrical parameters and no mechanical parameters such as rotor inertia and damping coefficient. Moreover, indirect flux in the stationary reference frame can be obtained via direct

calculation of the voltage equation without any integral operation. Thus the effect of mechanical parameters and integration drift can be reduced. However, the accuracy of sensorless estimation depends on the accuracy of electrical parameters. In particular, resistance of stator winding can be changed by temperature variations such as rising due to motor operation and so on.

This paper presents an accurate electrical parameter mea- surement and compensation method for high estimation performance of the sensorless PMSM.

Fig. 4 shows the general measurement technique for electrical parameters in an equivalent circuit of the PMSM in standstill. In standstill, back emf can be ignored by the pulse voltage and the phase current can be expressed as a exponential function of electrical parameters, such as inductance and resistance shown in Fig. 4(b). For accurate measurement of electrical parameters, precise current sensing is essential. However, a digital controller based on DSP can detect the transient phase current only one or two times in a pulse period. In a short pulse period, on-line measurement of transient phase current has some problem for insufficient current detecting data.

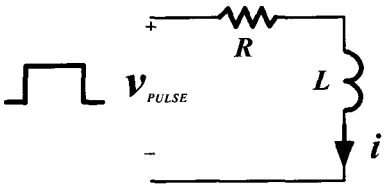

(a) Equivalent circuit of PMSM in standstill

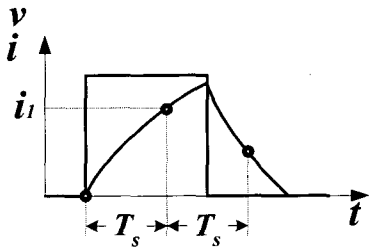

(b) Applied test pulse and current waveform

Fig. 4 A basic concept of parameter measurement

In this paper, a TCM using on-line FFT analysis is proposed for accurate measurement of electrical parameters. Fig. 5 shows the analytical model of the proposed TCM using on-line FFT analysis. To obtain a large amount of data from the signal source during a limited period as shown in Fig. 5(a), the concept of time extension is required. In this paper, an LPF is used for time extension. The transfer function ***H(s)*** denotes the LPF for time extension in Fig. 5. The signals i' and v' denote filtered signals of phase current and applied pulse voltage respectively. The time expended signals of the LPF have to be sensed by the DSP controller to achieve more data.

The proposed TCM with FFT analysis is used to obtain the accurate orignal signal. To return its original signal from the sampled data, the output signals i' and v' are first implemented on the FFT analysis. The FFT results become the means to describe them as sinusoidal equations. The retraced signal i_E of the orignal phase current can be obtained as a summation of the inverse function, $H(jw_n)^{-1}$ of ***H(s)*** in frequency domain and filtered output signal i'. Therefore, electrical parameters L_n and R_n in all frequency regions can be calculated by the FFT analyzed signals of i' and v'. The DSP controller can precisely calculate electrical parameters ***L*** and ***R*** by the LMS method for the sensorless control algorithm. Fig. 5(b) shows the block diagram of the proposed TCM for the accurate measurement of electrical parameters.

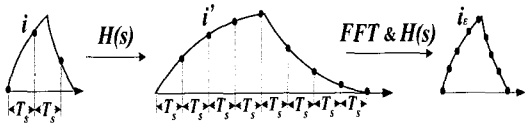

(a) Time extended current signal

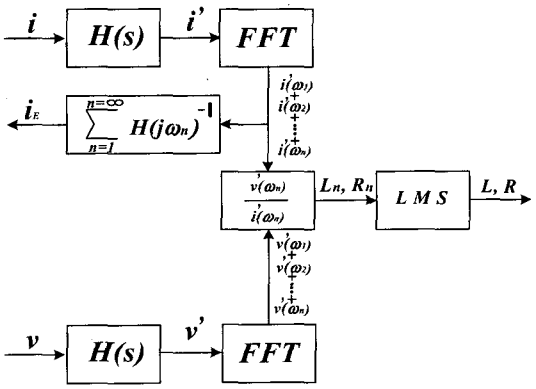

(b) Current recovery and parameter calculation

Fig. 5 A concept of the proposed TCM

Fig. 6 shows the analog LPF for the phase current. The second order analog LPF is designed for phase current. The digital LPF for applied pulse voltage is implemented to reduce A/D converter.

The transfer function of the designed second-order LPF is

$$H(s) = \frac{G_o b}{s^2 + as + b} \tag{17}$$

$$G_o = -\frac{R_2}{R_1}$$
$$a = \frac{1}{C_1}\left(\frac{1}{R_1} + \frac{1}{R_2} + \frac{1}{R_3}\right)$$
$$b = \frac{1}{C_1 C_2 R_2 R_3}. \tag{18}$$

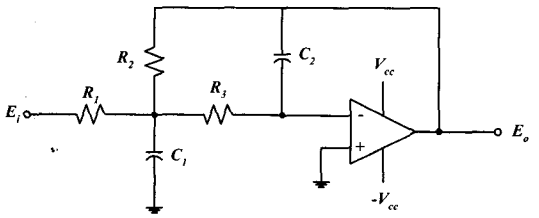

Fig. 6 Designed second-order LPF

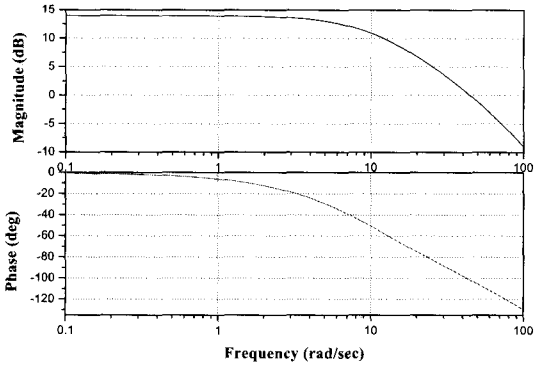

Fig. 7 Bode plot of the designed LPF

Fig. 7 shows the bode plot with values of G_o=5, a=110, b=1000, respectively. To increase the precision, G_o should be determined considering the variable displacement of the employed A/D converter. a and b should be determined by the cut-off frequency of the LPF. The cut-off frequency of the LPF becomes 10Hz as shown in Fig. 7. From the retraced signal and applied pulse voltage, motor parameters $\boldsymbol{R}$ and $\boldsymbol{L}$ can be obtained, respectively. Although they can theoretically be calculated by voltage and current at a certain frequency, to obtain more accurate motor parameters the following procedure should be required. Motor parameters are obtained at every frequency, and the LMS is adapted to the data. Of course, measurement error should be considered.

3.2 Compensation of Temperature Effect

The accurate electrical parameters can be obtained by the proposed TCM. However, FFT analysis of the TCM requires a large calculation time. For this reason, the proposed TCM is used only before starting and can not be implemented at an instant sampling period in the operating region. For instantaneous compensation for parameter variation due to temperature in the operating region, a simple compensation method is used. The time-constant of the temperature variation becomes considerably larger than any other variations in the overall system. Because the initial motor parameters can be precisely obtained by the proposed TCM, the practical parameter variation by the temperature has a long time-constant. Fig. 8 shows the proposed parameter compensation method, which uses the error between the instantaneous estimated rotor speed and the average calculated reference speed from the reference angle per revolution. Practically, the DSP timer 1 interrupter is used to calculate the average reference speed. The PI compensator can compensate for motor parameter in every sampling period. With the proposed TCM for accurate detecting of motor parameters and a simple parameter compensator, a robust sensorless estimation is possible.

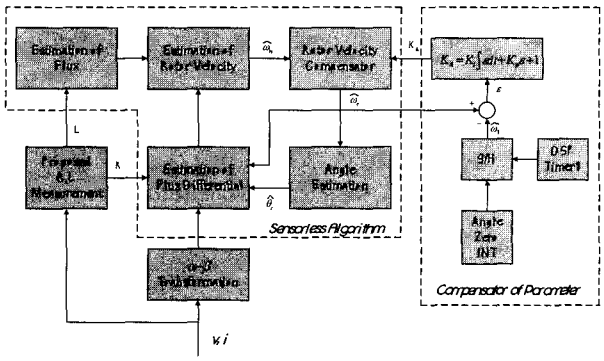

Fig. 8 Block diagram of rotor speed and angle estimation

4. Experimental Results

To verify the proposed sensorless algorithm, an experimental test is implemented. A DSP controller with TMS320F240 is used for estimation and speed control of the PMSM. The phase currents are measured in a ten-bit A/D converter by the current sensor via an appropriate filter to reduce the high frequency harmonic components. To compare the actual and estimated value, an optical shaft encoder was used.

Fig. 9 shows the overall block diagram of the sensorless speed control of the PMSM. Angular velocity and position are estimated in the stationary reference frame with measured phase current and electrical parameters from the TCM. The outer PI speed controller and inner current controller control the rotor speed and phase current respectively. The speed controller has an 1 ㎳ sampling period. The sampling period of the inner loop current controller is designed with a 200μs. SVPWM technique is used to produce the actual switching voltage. In the experiment, a 1.2 Kw surface mounted PMSM is used. Fig. 10 shows the experimental constructions and designed controller.

The starting performance of the proposed sensorless speed control algorithm is tested in the case of initial position error. Fig. 11 shows the sensorless speed response and position estimation in case of 45° and 85° initial position errors respectively. With the initial position error, the proposed sensorless algorithm can estimate the accurate rotor position stably.

Table 1 shows the specification of tested PMSM.

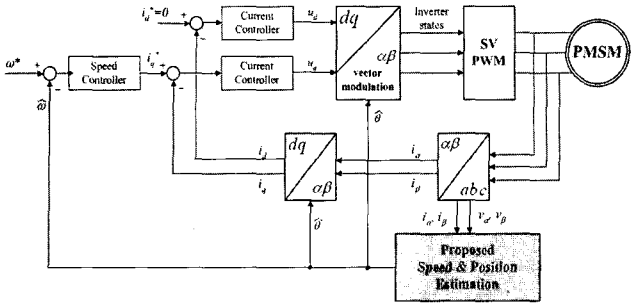

Fig. 9 Block diagram of sensorless speed control

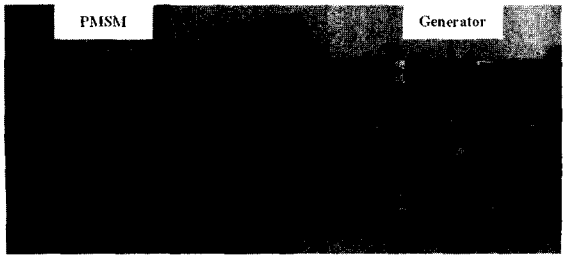

(a) PMSM and generator system

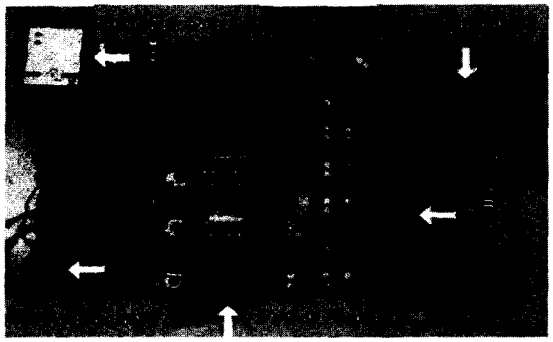

(b) Sensor and power system

Fig. 10 Experimental constructions

Table 1 The specification of tested PMSM

Winding resistance	0.8 Ω
Winding inductance	0.92 mH
Max. value of the flux linkage	0.051 Wb.t
Number of poles	4
Rated current	6.2 A
Rated Speed	3,000 rpm

Fig. 12 shows the experimental results in the low speed region case. The tested PMSM has rated speed of 3,000 rpm. Under 30 rpm and 21 rpm reference speed those are 1.0% and 0.7% of rated speed condition are tested respectively. Experimental results at less than 1% of the rated speed show stable sensorless speed control and accurate estimation of the rotor position.

Fig. 13 shows the phase current and sensorless speed response with the load disturbance. The disturbance load was changed from 1.5 Nm to 3.0 Nm. With the step changing of the disturbance load, the proposed sensorless algorithm can keep track of the reference speed.

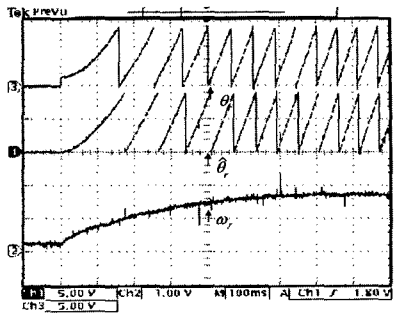

(a) 45° position error

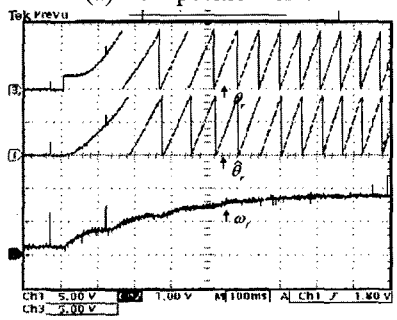

(b) 85° position error

Fig. 11 Sensorless speed response with initial position error

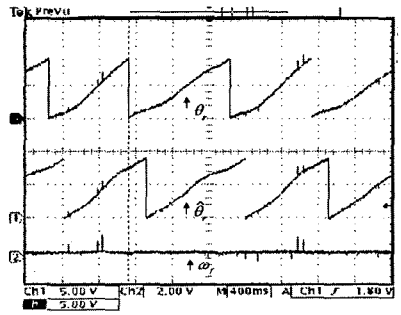

(a) 30 rpm reference speed

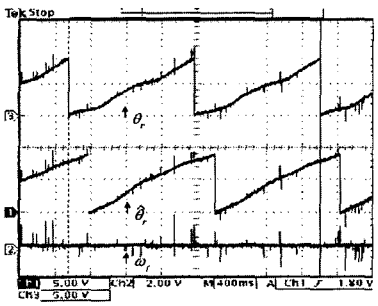

(b) 21 rpm reference speed

Fig. 12 Sensorless speed response in the low speed region

Fig. 14 shows the experimental results with a reference speed change. Fig. 14 (a) shows the reference speed and the actual speed when the reference speed changes from 1,000 rpm to 2000 rpm. Fig. 14 (b) is the experimental result of a reference speed change from 1000 rpm to

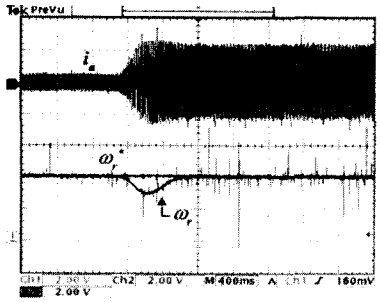

(a) Load changing from 1.5 rpm to 3.0 Nm

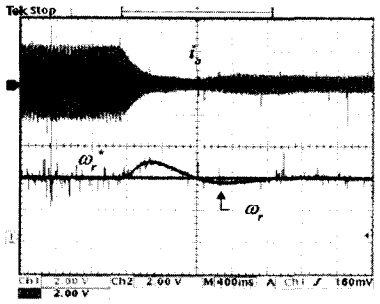

(b) Load change from 3.0 Nm to 1.5 Nm

Fig. 13 Experimental results in the case of sudden load change

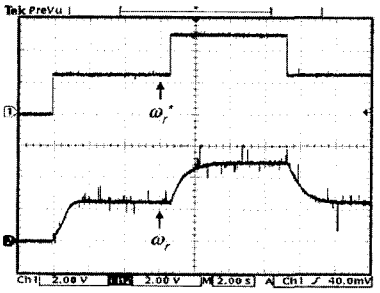

(a) In case of ω_r^* changing from 1000 rpm to 2000 rpm

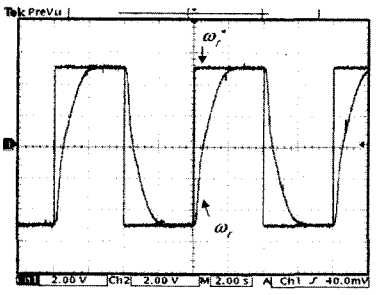

(b) In case of ω_r^* changing from 1000 rpm to -1000 rpm

Fig. 14 Experimental results with reference speed changing

-1000 rpm. With a sudden change of reference speed and direction, the proposed algorithm can well keep track of the reference speed according to the experimental results.

Fig. 15 shows the operating performance of the proposed sensorless algorithm in the case of rated speed reference and rated load conditions.

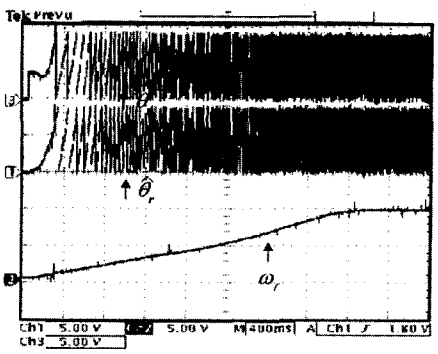

Fig. 15 Sensorless control performance in the case of rated speed and load conditions

After several sampling periods, the estimated rotor position keep track of the actual rotor position well while the DSP controller has the initial rotor position error.

To verify the proposed sensorless algorithm, tests are run with starting characteristics of initial position error, speed response in low speed region, load disturbance, sudden change of reference speed, and rated condition. These experimental results show that the proposed indirect flux detecting method with TCM can estimate well the actual rotor position and robust control performance.

5. Conclusions

A simple and stable position sensorless control strategy for a PMSM was presented in this paper. A speed control scheme was based on the indirect flux detecting method with no any integral operation. The rotor position and speed were estimated through estimation of the magnetic flux and differential magnetic field with a simple rejection technique for switching noise effect. Magnetic flux and differential magnetic field were calculated by indirect flux detecting method, and the angular velocity can be derived from the magnetic flux and differential magnetic field. In addition, to compensate the estimation error from nonlinear characteristics of voltage equation, a compensation term is added to estimate the rotor position. The error term is for continuous compensation of estimation error and robust sensorless control.

To accurately estimate the rotor position, a direct measurement method is adapted using the time-compression method and a compensation technique for temperature variation. The closed-loop sensorless speed control has been shown to be effective from standstill to rated speed and during a sudden load disturbance. Moreover, in a very low speed range, the proposed sensorless algorithm can well keep track of the reference speed.

References

[1] K. Iizuka et al., "Microcomputer Control for Sensorless Brushless Motor," *IEEE Trans. on Industry Applications*, vol. IA-27, pp. 595-601, 1985.

[2] Peter Vas, *Sensorless Vector and Direct Torque Control*, Oxford Univ., 1998.

[3] N. Matsui, "Sensorless PM Brushless DC Motor Drives," *IEEE Trans. on Industrial Electronics*, vol. 43, no. 2, pp.300-308, 1996.

[4] J. Oyama, T. Abe, T. Higuchi, E. Yamada, "A Nonlinear Reduced Order Observer for Permanent Magnet Synchronous Motors," *IEEE Trans. on Industrial Electronics*, vol.43, pp.38-43, August, 1996.

[5] Silverio Bolognani, Robert Oboe and Mauro Ziliotto, "Sensorless Full-Digital PMSM Drive With EKF Estimation of Speed and Rotor Position", *IEEE Trans. on Industrial Electronics*, vol. 46, no. 1, pp. 184-191, February, 1999.

[6] J. S. Kim and S. K. Sul, "High Performance PMSM Drives without Rotational Position Sensors using Reduced Order Observer," *Record of the 1995 IEEE Industry Applications Conf.*, vol. 1, pp.75-82, 1995.

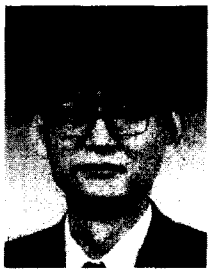

Tae-Hyun Won was born in Busan, Korea, in 1965. He received the B.S. and M.S. degrees in Electrical Engineering from Pusan National University in 1986 and 1988, respectively, and the Ph.D. degree in Mechatronics Engineering from Pusan National University in 2002. He worked at the Agency for Defence Development from 1988 to 1997. Since 1998, he has been with the Department of Electrical Engineering, Dongeui Institute of Technology, Korea. His research interests are mechatronics, intelligent control, motor control, and power electronics. He is a member of KIEE, ICASE, and KSME.

Man Hyung Lee was born in Korea in 1946. He received the B.S. and M.S. degrees in Electrical Engineering from Pusan National University, Korea, in 1969 and 1971, respectively, and the Ph.D. degree in Electrical and Computer Engineering from Oregon State University, Corvallis, in 1983. From 1971 to 1974, he was an instructor in the Department of Electronics Engineering, Korea Military Academy. He was an assistant professor in the Department of Mechanical Engineering, Pusan National University, from 1974 to 1978. From 1978 to 1983, he held positions as a teaching assistant, research assistant, and postdoctoral fellow at Oregon State University. Since 1983, he has been a professor in the College of Engineering, Pusan National University, where he is also currently POSCO Chair Professor in the School of Mechanical Engineering. His research interests are estimation, identification, stochastic processes, bilinear systems, mechatronics, micromachine automation, and robotics. He is the author of more than 550 technical papers and was General Co-Chairmen of the ISIE 2001.

Dr. Lee is a senior member of IEEE, a member of the American Society of Mechanical Engineers, the Society for Industrial and Applied Mathematics, and the Society of Photo-Optical Instrumentation Engineers.